

Damage-resistant alumina-based layer composites

Linan An and Helen M. Chan

Department of Materials Science and Engineering, Lehigh University, Bethlehem, Pennsylvania 18015

Nitin P. Padture^{a)} and Brian R. Lawn

Materials Science and Engineering Laboratory, National Institute of Standards and Technology, Gaithersburg, Maryland 20899

(Received 16 March 1995; accepted 25 August 1995)

A new philosophy for tailoring layer composites for damage resistance is developed, specifically for alumina-based ceramics. The underlying key to the approach is microstructural control in the adjacent layers, alternating a traditional *homogeneous* fine-grain alumina (layer **A**) for hardness and wear resistance with a *heterogeneous* alumina:calcium-hexaluminate composite (layer **C**) for toughness and crack dispersion, with strong bonding between the interlayers. Two trilayer sequences, **ACA** and **CAC**, are investigated. Hertzian indentation tests are used to demonstrate the capacity of the trilayers to absorb damage. In the constituent materials, the indentation responses are fundamentally different: ideally brittle in material **A**, with classical cone cracking outside the contact; quasi-plastic in material **C**, with distributed microdamage beneath the contact. In the **ACA** laminates, shallow cone cracks form in the outer **A** layer, together with a partial microdamage zone in the inner **C** layer. A feature of the cone cracking is that it is substantially shallower than in the bulk **A** specimens and does not penetrate to the underlayer, even when the applied load is increased. This indicates that the subsurface microdamage absorbs significant energy from the applied loads, and thereby “shields” the surface cone crack. Comparative tests on **CAC** laminates show a constrained microdamage zone in the outer **C** layer, with no cone crack, again indicating some kind of shielding. Importantly, interlayer delamination plays no role in either layer configuration; the mechanism of damage control is by crack suppression rather than by deflection. Implications for the design of synergistic microstructures for damage-resistant laminates are considered.

I. INTRODUCTION

Laminates have been developed as a means of containing crack propagation in tension or bending, principally by delamination along an orthogonal path. Such delamination cracks lend themselves to analysis by engineering mechanics, essentially by regarding adjacent layers as continuum slabs bonded by weak interfaces and treating the failure as an interfacial delamination.¹⁻⁴ However, deflection cracks can cause problems of their own and lead to premature failures in alternative loading states (e.g., in bending or compression), as well as to the destruction of other critical (e.g., electronic, thermal) functions. In this context, it is perhaps curious that so little attention has been given to microstructural tailoring for general improvement in crack suppression by damage accumulation, and specific avoidance of

delamination cracks. Preliminary steps in this direction have been taken in our laboratories in the fabrication of duplex and laminar ceramic composites for enhanced flaw tolerance.^{5,6} Marshall and co-workers have also used microstructural design concepts to develop high-toughness alumina-based composites: alumina/zirconia, where layer thickness constraints dictate the shape and size of transformation zones in toughened Cey-TZP layers,^{7,8} and alumina/monazite, where the monazite acts as a weak phase not only for crack deflection but also, to some extent, crack arrest.⁹

Here we consider a new approach, in which microstructural elements are designed to provide a fundamentally different mode of crack control. The basic idea is to alternate ceramic layers with homogeneous microstructures, designed for hardness and wear resistance, and heterogeneous microstructures, designed for toughness and damage dispersion. Adjoining interfaces are strongly bonded to avoid delamination. The motivation for this philosophy comes from recent

^{a)}Now at Department of Metallurgy and Institute of Materials Science, University of Connecticut, Storrs, Connecticut 06269.

observations of damage patterns in newer-generation polycrystalline ceramics with weak grain boundaries, coarse grains, and high internal stresses, so-called “heterogeneous” ceramics,¹⁰ using Hertzian indentation as a diagnostic tool. In traditional “homogeneous” brittle solids like glasses, single crystals, and fine-grain polycrystalline ceramics, Hertzian indentation produces classical cone fractures outside the contact circle.^{10–24} In “heterogeneous” ceramics the indentation damage is of an altogether different kind, consisting of a diffuse damage zone beneath the contact.^{25–34} The latter damage is shear driven, and operates discretely at the microstructural level in the form of “shear faults” along localized weak planes, e.g., grain or interphase boundaries. The integrated effect of these discrete events over the damage zone is manifested as a macroscopic quasiductility.²⁷ Accordingly, heterogeneous ceramics of this kind emerge as attractive candidates for incorporation as alternate layers in laminate structures, for dispersion of potentially dangerous cracks.

The present paper represents a first attempt to demonstrate the effectiveness of this alternative philosophy to crack containment. Accordingly, a Hertzian indentation study is made of model alumina-based trilayers consisting of homogeneous and heterogeneous components: for the homogeneous layers, a traditional fine-grain alumina; for the heterogeneous layers, a composite of matrix alumina grains and second-phase calcium-hexaluminate platelets.³⁵ Whereas earlier Hertzian indentation tests have shown that bulk fine-grain alumina undergoes classical cone-cracking,^{25,26} preliminary comparative tests on the bulk two-phase material indicate a distinctive diffuse damage zone from microfailure at the interphase boundaries (see Ref. 36). From the processing standpoint, these two alumina-based material components are ideally suited to formation of laminates, since each may be sintered to high density using the same heat treatments, and the two are structurally and thermodynamically stable when in contact. Conveniently, the two materials have similar thermal expansion coefficients, so that one may investigate the role of microstructure in the damage response without complication from macroscopic residual stresses. We shall show that when the homogeneous material constitutes the outer layer, a shallow cone crack forms around the Hertzian contact, but is inhibited from penetrating the interface by the simultaneous formation of distributed damage in the inner layer. When the heterogeneous material constitutes the outer layer, distributed damage forms in this layer, but is constrained from developing into the subsurface; in this case cone cracking in either layer is suppressed. The results suggest an interlayer synergism, in which the damage process in one layer “shields” the countervailing process in the adjacent layer.

II. TRILAYER PREPARATION AND CHARACTERIZATION

A. Preparation

Alumina (Al_2O_3) and alumina:calcium-hexaluminate ($\text{Al}_2\text{O}_3:\text{CaAl}_2\text{O}_6$) were first processed as separate samples for baseline testing. Alumina was prepared using high purity, submicrometer powder (Sumitomo, AKP-HP, Osaka, Japan). Alumina:calcium-hexaluminate was formed by reaction-sintering a mixture of alumina and calcium carbonate (Alfa 10996, Johnson Matthey, Ward Hill, MA) powders, in a mix designed to form 30 vol% calcium hexaluminate in the final composition, with 1 vol% anorthite glass ($\text{CaO} \cdot \text{Al}_2\text{O}_3 \cdot 2\text{SiO}_2$) as a sintering additive.³⁵

Both the alumina and the alumina:calcium-hexaluminate starting powders were individually ball milled into slurries in methanol for 24 h, using zirconia ball grinding media. The slurries were subsequently dried while subjected to continuous mixing on a stirrer/hot plate. After drying, the caked powders were uniaxially die-pressed at 50 MPa, followed by isostatic pressing at 350 MPa. The green pellets were then calcined at 1400 °C for 24 h, followed by sintering at 1600 °C for 1 h. For the alumina (designated **A**), this preparation schedule produced a homogeneous fine-grain microstructure with relatively well-bonded grain boundaries; for the alumina:calcium-hexaluminate (designated **C**), it produced a heterogeneous microstructure with elongate platelike hexaluminate grains and weak interphase boundaries.³⁵

Laminate specimens were then prepared by introducing the appropriate powder mixes into the die in three separate layers, in both **ACA** and **CAC** sequences as depicted in Fig. 1. The trilayer configuration was chosen so as to avoid any specimen warping from sintering stresses. Subsequent heat-treatment conditions were the same as those above for the individual materials. The net thickness of the sintered trilayer specimens was ≈ 4 mm, with individual outer layers ≈ 1 mm. The as-

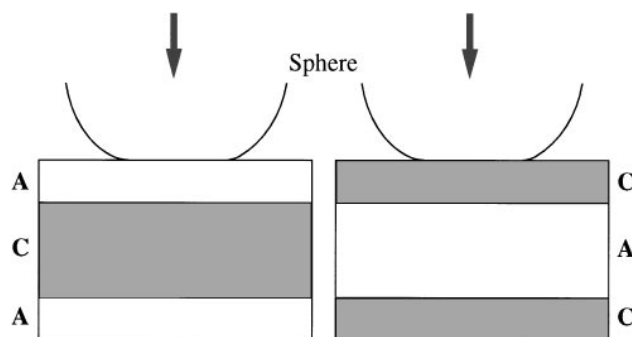
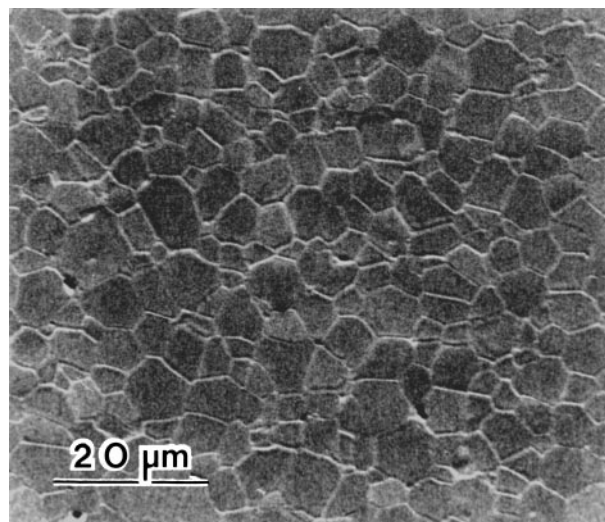


FIG. 1. Trilayer composite structures subjected to Hertzian indentation: A, alumina; C, alumina:calcium-hexaluminate.

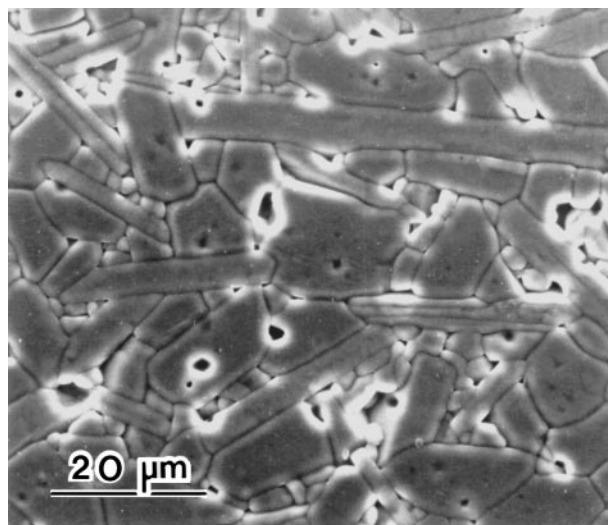
fired surfaces were then ground to reduce the outer layer thickness to $\approx 200\text{--}300\ \mu\text{m}$.

B. Characterization

Microstructural characterization was carried out on the fired specimens. Surfaces were polished to $1\ \mu\text{m}$ finish, thermally etched at $1400\ ^\circ\text{C}$ for 1 h, and gold-coated for examination in a scanning electron microscope (SEM). SEM micrographs for the alumina and alumina:calcium-hexaluminate composite materials are shown in Figs. 2(a) and 2 (b), respectively. The alumina has a uniform, equiaxed grain structure, with an average



(a)



(b)

FIG. 2. Scanning electron micrograph showing microstructures of constituent trilayer materials. Polished specimens thermally etched in air at $1400\ ^\circ\text{C}$ for 1 h. (a) Homogeneous alumina. Note equiaxed fine-grain structure. (b) Heterogeneous alumina:calcium-hexaluminate. Calcium hexaluminate grains are the platelets (confirmed by Ca x-ray mapping³⁵).

grain size $\approx 2.5\ \mu\text{m}$. The composite consists of a volume fraction of 30 vol % calcium-hexaluminate platelets $\approx 30\ \mu\text{m}$ long and $\approx 4\ \mu\text{m}$ wide dispersed in a fine-grain alumina matrix.³⁵

For the laminates, microscopic observations were made on the section surfaces to examine the interface region. The layers retained basically the same structure as the bulk constituent materials, other than a coarsening of the alumina grains to $\approx 30\ \mu\text{m}$ (cf. $\approx 2.5\ \mu\text{m}$ in bulk) across otherwise well-defined interfaces³⁵ (see optical micrographs below, Fig. 4). This latter coarsening is attributable to a local increase in calcium concentration from the adjoining C layer material.³⁷ To detect any spurious macroscopic residual stresses in the trilayers from either differential thermal expansion or the sintering process, Vickers indentations were placed wholly within the layers on the side surfaces, with radial arms parallel and perpendicular to the interfaces. In all cases the two sets of radial cracks remained straight and showed no significant differences in length (to within $\approx 2\%$), confirming the absence of significant stresses.

The Vickers indentations also provided a measure of grain boundary weakness, via the degree of intergranular fracture along the radial cracks: $\approx 60\%$ for alumina, virtually 100% for alumina:calcium-hexaluminate. Grain bridging was observed along the crack arms, especially at the calcium hexaluminate grains in the composite material, indicative of a toughness curve.

III. HERTZIAN CONTACT TEST

A. Test procedure

Contact damage was induced in the outer polished surfaces of both the individual A and C materials and the CAC and ACA trilayers using a tungsten carbide sphere of radius 3.18 mm, at peak normal loads up to 3000 N in air. After indentation, the damage sites were gold-coated and viewed in Nomarski interference contrast.

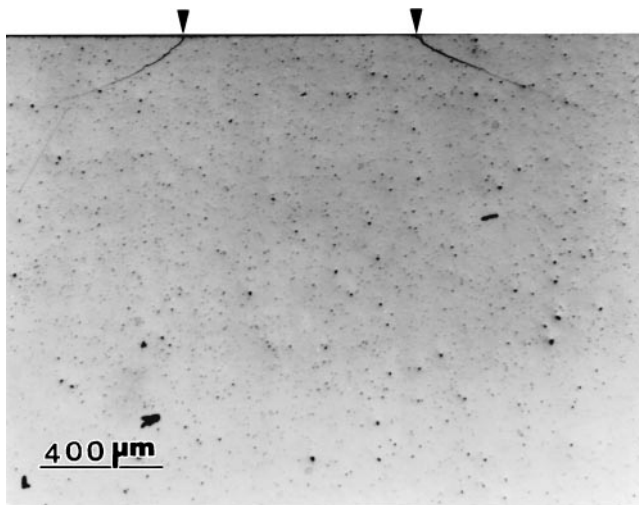
More detailed information on the subsurface damage morphology was obtained using a bonded-interface specimen configuration first introduced by Mulhearn for metals³⁸ and later adapted for ceramics by Guiberteau *et al.*²⁶ Thus, the faces of two half blocks were bonded together using a cyanoacrylate-based adhesive (Super Glue, Loctite Corp., Newington, CT). These half blocks were prepared by cutting any given specimen into two near-identical halves and polishing the opposing faces; for the laminates, the cut was made so that the bonded interface was normal to the internal laminate interfaces. After repolishing the top surface, a series of Hertzian indentations was made symmetrically across the bonded-interface trace. The two specimen halves were then separated by soaking in acetone to dissolve the adhesive, cleaned, and gold-coated for viewing in Nomarski contrast.

B. Results

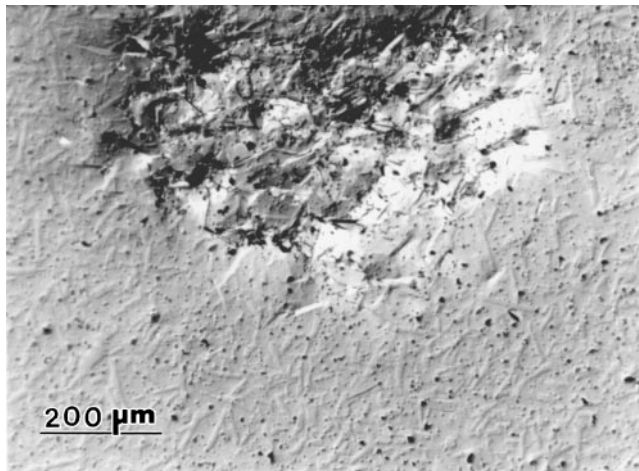
Subsurface Hertzian damage patterns are shown for the bulk **A** and **C** materials in Fig. 3, for indentation load 2000 N. In the homogeneous fine-grain alumina, Fig. 3(a), the damage takes the form of classical cone cracking, as observed in previous studies.^{25,26} In the heterogeneous alumina:calcium-hexaluminate composite material, Fig. 3(b), an altogether different form of damage is observed, namely a diffuse damage zone. Higher magnification examination of this latter damage zone in the SEM revealed a distribution of discrete microfailures by shear faulting at the weak boundaries between the elongate calcium-hexaluminate/alumina interphase boundaries, in the subsurface region of high

shear stress concentrations.³⁶ This type of shear fault damage is similar to that reported in other ceramic platelet composites.^{28–30,34} The same weak boundaries responsible for the shear faulting also act to suppress cone fracture, by deflecting any incipient surface ring cracks away from the highly directional tensile stress trajectories in their immediate downward propagation.²⁶ Hence the addition of microstructural heterogeneity effects a transition from a brittle (macroscopic tensile-driven cone crack) to a quasiductile (microscopic shear-driven shear faults) response.²⁷

Comparative Hertzian indentation responses for the **ACA** and **CAC** trilayers are shown in Fig. 4, again for indentation load 2000 N. Consider the **ACA** system first,

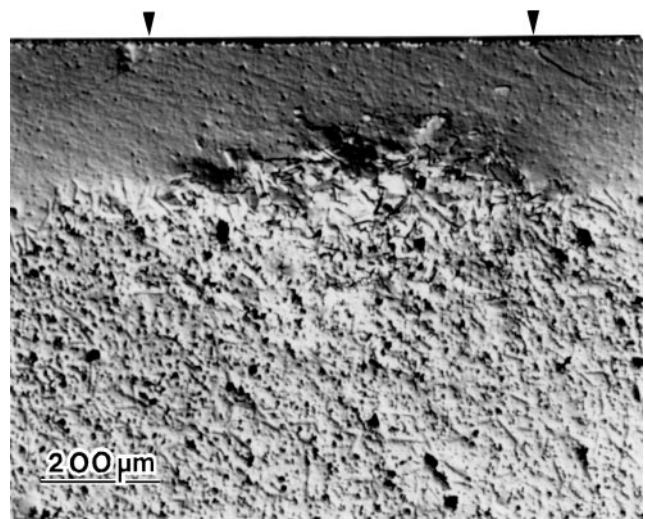


(a)

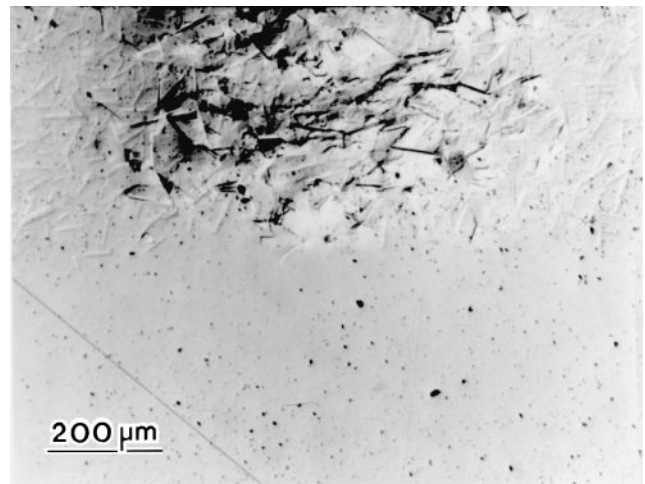


(b)

FIG. 3. Optical micrographs in Nomarski illumination showing section views of Hertzian contact sites in constituent layer **A** and **C** materials: (a) **A**, alumina; (b) **C**, alumina:calcium-hexaluminate. Indentations made using tungsten carbide indenter, radius 3.18 mm, load 2000 N. Arrows in (a) indicate surface cone crack. [Note different magnification in micrographs, lower in (a) to show entire cone crack.]



(a)



(b)

FIG. 4. Optical micrographs in Nomarski illumination showing section views of Hertzian contact sites in trilayer composites: (a) **ACA** and (b) **CAC**. Indentation conditions as in Fig. 3. Arrows in (a) indicate surface cone crack.

Fig. 4(a). A hybrid damage response is now apparent: cone-crack in the outer homogeneous **A** (alumina) layer, and subsurface shear fault zone in the heterogeneous **C** (alumina : calcium-hexaluminat) layer. These responses are similar in nature to those in the constituent bulk materials, but not in degree. The depth of cone-cracking in the outer layer is substantially smaller relative to the bulk alumina [$\approx 140 \mu\text{m}$ in Fig. 4(a) compared to $\approx 300 \mu\text{m}$ in Fig. 3(a)]. Likewise, the depth of distributed damage is smaller in the composite sublayer [$\approx 400 \mu\text{m}$ in Fig. 4(a) relative to $\approx 500 \mu\text{m}$ in Fig. 3(b)]; note, however, that this damage does extend back up into the outer layer, presumably due to the presence of the larger alumina grains in the interface region (Sec. II B). The suppression of the cone crack is of particular interest. Even on increasing the indentation load to 3000 N, Fig. 5, the surface cone crack barely increases in depth, and remains wholly contained in the outer layer; at the same time, the depth of damage in the sublayer increases. It therefore appears that the development of the subsurface damage zone has a marked shielding influence on the crack zone, wherein the stress buildup in the elastic-plastic field is constrained by a kind of “yield” limit. The degree of this shielding must ultimately be governed by the constitutive stress relations for initiation and subsequent evolution of the shear faults in the bulk quasiductile material. The role of microstructural parameters of the composite material in these constitutive relations,^{36,39} and of the thickness of the layers in the geometrical constraints, remain critical issues for study.

Now consider the **CAC** system, Fig. 4(b). In this case, there is no cone cracking in either component of the trilayer, and distributed shear fault damage is visible only

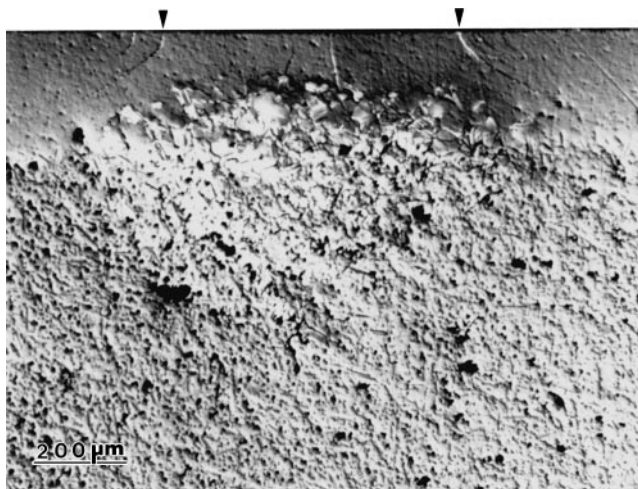


FIG. 5. Optical micrograph in Nomarski illumination showing section view of Hertzian contact sites in **ACA** laminar composite. Indentations made using tungsten carbide indenter, radius 3.18 mm, load 3000 N [cf. Fig. 4(a)]. Arrows indicate surface cone crack.

in the outer **C** (alumina : calcium-hexaluminat) layer. The distributed damage appears to be of the same form as in the bulk [Fig. 3(b)], although now its depth is constrained by the thickness of the outer layer. Again, the formation of a “yield” zone evidently dampens buildup of tensile stresses in the **A** sublayer, helping to suppress the development of internal cone-like fractures.

IV. DISCUSSION

The above Hertzian contact test results, particularly those in Fig. 4, suggest a hitherto unexplored route to ceramic layer design for controlling potentially deleterious surface damage from spurious stress concentrations. The novel aspect of the approach is the alternation of homogeneous and heterogeneous layers, the latter to absorb energy from the contact field by damage accumulation and the former to provide geometrical constraint for this damage mode. In the present study we have used trilayers of a traditional fine-grain alumina (**A**) and an alumina : calcium-hexaluminat composite (**C**) as a model illustrative system. In the **ACA** trilayer structure, the generation of a distributed shear-fault damage zone in the heterogeneous subsurface **C** layer greatly inhibits the extent of cone cracking in the homogeneous outer **A** layer. In the **CAC** structure, the development of a similar but now constrained damage zone in the outer layer suppresses cone fracture altogether (although it is probable that macroscopic fracture would develop from the shear fault zones at excessive contact loads^{16,34}). Mutual suppression in damage responses of the constituent ceramics is key to the inhibition of macroscopic cracking in the laminates. Central to the effectiveness of this suppression is an interlayer synergism, whereby the distributed damage process in the **C** layer “shields” the macroscopic cone fracture process in the **A** layer, and vice versa. In such a way, one may aspire to design layer structures with all the virtues, and hopefully none of the liabilities, of the two constituent materials.

In the context of this last point, it is interesting to contrast the proposed microstructural design philosophy with more traditional materials design concepts for ceramic laminate structures. It is customary to incorporate weakness at the interlayer level, to promote delamination and thereby inhibit normal tensile fracture,^{1,4} without close regard to the microstructures contained within the individual layers. It is then the interfacial energy that governs the failure properties. Some researchers have sought to counteract the brittleness by alternating ceramic with metal layers.⁴⁰ Others have sought to contain fracture by incorporating outer-layer residual compressive stresses from interlayer thermal expansion mismatch.⁴¹ Still other attempts have been made to tailor tough materials by enhancing crack deflections at weak internal boundaries, as in *in situ*-textured fibrous

composites.^{42–44} However, while all of these strategies are successful to a greater or lesser extent in suppressing normal fracture, they are simultaneously all susceptible to degradation from transverse fracture. Even ceramic/metal composites are susceptible to delamination from the relatively large elastic/plastic mismatch. In the philosophy proposed in the current work, transverse fracture is avoided by ensuring a strong bond between the alternating homogeneous and heterogeneous ceramic layers, without excessive interlayer mismatch. This is not to say that interfacial weakness is altogether eliminated from the structures; rather, such weakness is confined to the grain-facet scale within the heterogeneous layers, absorbing energy in these layers by damage accumulation at the microstructural level as a distribution of many discrete microfailures rather than a few well-defined macrocracks.

Given the role of mutual shielding by the damage processes in our proposed alternating homogeneous/heterogeneous structures, it is inevitable that layer thickness will be an important parameter in the composite design. The condition for effective shielding is that the stress field from concentrated loads on the outer surface should be sufficient to generate damage in the sublayer. This means that the layer thickness should be less than some characteristic contact diameter (but not so small that any desirable properties of the outer layer are rendered ineffective). In particular applications, therefore, it may therefore be necessary to custom-tailor layer thicknesses to the scale of prospective surface damage events, e.g., in bearing applications, impact, or scratching with inadvertent blunt or sharp particles. These may be important considerations in the design of coating/substrate and graded composites.

Finally, we may conjecture on various mechanical properties of our alumina-based layer structures:

(i) *Strength degradation.* By virtue of the strong bonding at the interlayer interfaces, loss of strength from delamination is no longer a serious threat. In fact, one might expect the degree of strength degradation from surface damage events to be smaller for the layer structures than for the bulk materials: in the **ACA** trilayers, because of the diminished scale of cone cracking [Fig. 4(a)]^{19,45–47}; in the **CAC** trilayers, because of the relatively innocuous flaws in the damage zone [Fig. 4(b)].²⁸

(ii) *Wear resistance.* Generally, the incorporation of microstructural heterogeneity into alumina and other ceramic microstructures degrades wear resistance.^{48,49} (Indeed, such heterogeneous microstructures have been proposed as effective routes to “machinable” ceramics.^{50,51}) In the **ACA** composite, the relatively high hardness and wear resistance of fine-grain alumina is not compromised by laminate formation (provided the outer layer is thick enough so that wear does not occur

down to the sublayer). Conversely, the **CAC** composite is highly susceptible to surface removal, and should be avoided in wear-resistant applications.

(iii) *Thermal shock and fatigue.* The introduction of heterogeneity provides scope for greater energy dissipation with a high density of distributed damage elements, specifically from internal frictional processes at individual shear faults.^{39,52} This can lead to enhancement of thermal shock resistance in thermal cycling,⁵³ but conversely to degradation of contact fatigue resistance in mechanical cycling.^{29,32,34}

(iv) *High temperature properties.* A feature of the alumina-based trilayers described here is their chemical compatibility and stability. They may therefore be expected to maintain their structural integrity at elevated temperatures, at least within a hundred degrees or so of the sintering temperature (1600 °C, Sec. II A). Such ceramic/ceramic structures are therefore likely to have greater lifetimes within the creep regime than other hybrid structures, such as ceramic/metal composites.⁴⁰

ACKNOWLEDGMENTS

This work was funded by the U.S. Air Force Office of Scientific research. Financial support from the Ford Motor Company for two of the authors (LA and HMC) is also acknowledged.

REFERENCES

1. K. Kendall, Proc. R. Soc. London A **344**, 287–302 (1975).
2. J. W. Hutchinson, in *Metal-Ceramic Interfaces*, edited by M. Rühle, A. G. Evans, M. F. Ashby, and J. P. Hirth (Acta-Scripta Metall. Proceedings Series, 1990), Vol. 4, pp. 295–306.
3. J. W. Hutchinson and Z. Suo, Adv. Appl. Mech. **29**, 64 (1991).
4. W. J. Clegg, K. Kendall, N. M. Alford, T. W. Button, and J. D. Birchall, Nature (London) **347**, 455–457 (1991).
5. C. J. Russo, M. P. Harmer, H. M. Chan, and G. A. Miller, J. Am. Ceram. Soc. **75**, 3396–3400 (1992).
6. M. P. Harmer, H. M. Chan, and G. A. Miller, J. Am. Ceram. Soc. **75**, 1715–1728 (1992).
7. D. B. Marshall, J. J. Ratto, and F. F. Lange, J. Am. Ceram. Soc. **74**, 2979–2987 (1991).
8. D. B. Marshall, Am. Ceram. Soc. Bull. **71**, 969–973 (1992).
9. P. E. D. Morgan and D. B. Marshall, J. Am. Ceram. Soc. (1995, in press).
10. B. R. Lawn, *Fracture of Brittle Solids* (Cambridge University Press, Cambridge, 1993).
11. F. C. Roesler, Proc. Phys. Soc. London B **69**, 981 (1956).
12. F. C. Frank and B. R. Lawn, Proc. R. Soc. London A **299**, 291–306 (1967).
13. B. R. Lawn, J. Appl. Phys. **39**, 4828–4836 (1968).
14. M. V. Swain and B. R. Lawn, Phys. Status Solidi **35**, 909–923 (1969).
15. T. R. Wilshaw, J. Phys. D: Appl. Phys. **4**, 1567–1581 (1971).
16. B. R. Lawn and T. R. Wilshaw, J. Mater. Sci. **10**, 1049–1081 (1975).
17. A. G. Evans and T. R. Wilshaw, Acta Metall. **24**, 939–956 (1976).
18. M. V. Swain and J. T. Hagan, J. Phys. D: Appl. Phys. **9**, 2201–2214 (1976).

19. B. R. Lawn and D. B. Marshall, in *Fracture Mechanics of Ceramics*, edited by R. C. Bradt, D. P. H. Hasselman, and F. F. Lange (Plenum, New York, 1978), Vol. 3, pp. 205–229.
20. R. Warren, *Acta Metall.* **26**, 1759–1769 (1978).
21. B. R. Lawn and S. M. Wiederhorn, in *Contact Mechanics and Wear of Rail/Wheel Systems*, edited by J. Kalousek, R. V. Dukkipati, and G. M. Gladwell (University of Waterloo Press, Vancouver, 1983), pp. 133–147.
22. K. Zeng, K. Breder, and D. J. Rowcliffe, *Acta Metall.* **40**, 2595–2600 (1992).
23. K. Zeng, K. Breder, and D. J. Rowcliffe, *Acta Metall.* **40**, 2601–2605 (1992).
24. J. S. Field and M. V. Swain, *J. Mater. Res.* **8**, 297–306 (1993).
25. F. Guiberteau, N. P. Padture, H. Cai, and B. R. Lawn, *Philos. Mag. A* **68**, 1003–1016 (1993).
26. F. Guiberteau, N. P. Padture, and B. R. Lawn, *J. Ceram. Soc.* **77**, 1825–1831 (1994).
27. B. R. Lawn, N. P. Padture, H. Cai, and F. Guiberteau, *Science* **263**, 1114–1116 (1994).
28. H. Cai, M. A. Stevens Kalceff, and B. R. Lawn, *J. Mater. Res.* **9**, 762–770 (1994).
29. H. Cai, M. A. S. Kalceff, B. M. Hooks, B. R. Lawn, and K. Chyung, *J. Mater. Res.* **9**, 2654–2661 (1994).
30. N. P. Padture and B. R. Lawn, *J. Am. Ceram. Soc.* **77**, 2518–2522 (1994).
31. A. Pajares, F. Guiberteau, B. R. Lawn, and S. Lathabai, *J. Am. Ceram. Soc.* **78**, 1083–1086 (1995).
32. A. Pajares, L. Wei, B. R. Lawn, and D. B. Marshall, *J. Mater. Res.* **10**, 2613 (1995).
33. H. H. K. Xu, L. Wei, N. P. Padture, B. R. Lawn, and R. L. Yeckley, *J. Mater. Sci.* **30**, 869–878 (1995).
34. N. P. Padture and B. R. Lawn, *J. Am. Ceram. Soc.* **78**, 1431–1438 (1995).
35. L. An, K. Soni and H. M. Chan, *J. Mater. Sci.* (1995, in press).
36. L. An and H. M. Chan, in N. P. Padture and B. R. Lawn, *Acta Metall.* **43**, 1609–1617.
37. S. I. Bae and S. Baik, *J. Am. Ceram. Soc.* **76**, 1065–1067 (1993).
38. T. O. Mulhearn, *J. Mech. Phys. Solids* **7**, 85–96 (1959).
39. A. C. Fischer-Cripps and B. R. Lawn, *Acta Metall.* (in press).
40. M. C. Shaw, D. B. Marshall, M. S. Dadkhah, and A. G. Evans, *Acta Metall.* **41**, 3311–3322 (1993).
41. R. Sathyamoorthy, A. V. Virkar and R. A. Cutler, *J. Am. Ceram. Soc.* **75**, 1136–1141 (1992).
42. S. Baskaran, S. D. Nunn, D. Popovic, and J. W. Halloran, *J. Am. Ceram. Soc.* **76**, 2209–2216 (1993).
43. S. Baskaran and J. W. Halloran, *J. Am. Ceram. Soc.* **76**, 2217–2224 (1993).
44. S. Baskaran and J. W. Halloran, *J. Am. Ceram. Soc.* **76**, 1249–1255 (1994).
45. B. R. Lawn, S. M. Wiederhorn, and H. Johnson, *J. Am. Ceram. Soc.* **58**, 428–432 (1975).
46. S. M. Wiederhorn and B. R. Lawn, *J. Am. Ceram. Soc.* **60**, 451–458 (1977).
47. D. B. Marshall and B. R. Lawn, *J. Am. Ceram. Soc.* **61**, 21–27 (1978).
48. H. H. K. Xu and S. Jahanmir, *J. Am. Ceram. Soc.* **78**, 497–500 (1995).
49. H. H. K. Xu and S. Jahanmir, *J. Mater. Sci.* (1995, in press).
50. C. K. Chyung, G. H. Beall, and D. G. Grossman, in *Electron Microscopy and Structure of Materials*, edited by G. Thomas, R. M. Fulrath, and R. M. Fisher (University of California Press, Berkeley, CA, 1972), pp. 1167–1194.
51. N. P. Padture, C. J. Evans, H. H. K. Xu, and B. R. Lawn, *J. Am. Ceram. Soc.* **78**, 215–217 (1995).
52. B. R. Lawn, N. P. Padture, F. Guiberteau, and H. Cai, *Acta Metall.* **42**, 1683–1693 (1994).
53. K. Chyung, in *Fracture Mechanics of Ceramics*, edited by R. C. Bradt, D. P. H. Hasselman, and F. F. Lange (Plenum Press, New York, 1974), Vol. 2, pp. 495–508.